Society for Mathematical Biology

CrossMark

ORIGINAL ARTICLE

Mathematical Modeling of the Effects of Tumor Heterogeneity on the Efficiency of Radiation Treatment Schedule

Farinaz Forouzannia[1] · **Heiko Enderling[2]** · **Mohammad Kohandel[1]**

Abstract Radiotherapy uses high doses of energy to eradicate cancer cells and control tumors. Various treatment schedules have been developed and tried in clinical trials, yet significant obstacles remain to improving the radiotherapy fractionation. Genetic and non-genetic cellular diversity within tumors can lead to different radiosensitivity among cancer cells that can affect radiation treatment outcome. We propose a minimal mathematical model to study the effect of tumor heterogeneity and repair in different radiation treatment schedules. We perform stochastic and deterministic simulations to estimate model parameters using available experimental data. Our results suggest that gross tumor volume reduction is insufficient to control the disease if a fraction of radioresistant cells survives therapy. If cure cannot be achieved, protocols should balance volume reduction with minimal selection for radioresistant cells. We show that the most efficient treatment schedule is dependent on biology and model parameter values and, therefore, emphasize the need for careful tumor-specific model calibration before clinically actionable conclusions can be drawn.

✉ Farinaz Forouzannia
f3forouz@uwaterloo.ca

✉ Mohammad Kohandel
kohandel@uwaterloo.ca

Heiko Enderling
heiko.enderling@moffitt.org

[1] Department of Applied Mathematics, University of Waterloo, Waterloo, ON N2L 3G1, Canada

[2] Department of Integrated Mathematical Oncology, Department of Radiation Oncology, H. Lee Moffitt Cancer Center and Research Institute, Tampa, FL 33647, USA

1 Introduction

Radiation is commonly used in cancer treatment, either as monotherapy or as combination treatment with surgery and chemotherapy. Radiation is a DNA damaging agent, and radiation as cancer therapy benefits from cancer cells being less efficient in repairing radiation-induced damage than normal cells. Total radiation dose is divided into small frequent fractions to provide temporal windows for normal tissue recovery. Treatment schedules (fractionation) are predominantly based on evolved empirical knowledge and wisdom, but greatly constrained by logistical considerations. Recent developments include hypo- and hyperfractionation for various cancer types, that is delivery of either larger doses temporally further separated or smaller doses more frequently.

Despite many technical improvements in the efficiency of radiotherapy, many tumors are refractory to irradiation. Various clinical and biological factors explain such complications, including DNA damage repair (Hall and Giaccia 2006; Mathews et al. 2013), prevalence of hypoxia, and tumor heterogeneity and plasticity. Recently, the presence of cancer stem cells and a tumor hierarchy has been discussed as source of intratumoral heterogeneity and therapy response (Marjanovic et al. 2013; Shackleton et al. 2009). The cancer stem cell hypothesis proposes that the small subpopulation of so-called cancer stem cells (CSCs) is critically important for the initiation and maintenance of the tumor. These CSCs are able to self-renew indefinitely and undergo symmetric and asymmetric divisions to retrospectively increase the CSC population and produce progenitor cells that will make up the bulk of the tumor (Reya et al. 2001). Recent evidence suggests plasticity between non-CSC and CSC states (Gupta et al. 2011), due to genetic or microenvironmental perturbations. CSCs have been shown to utilize superior radiation-induced DNA damage repair mechanisms to prevent cell death (Bao et al. 2006). After radiation exposure, cells with damaged DNA attempt different pathways of repair, and the repair time is likely dependent on the delivered radiation dose (Lagadec et al. 2010; Sarcar et al. 2011).

The conventional radiotherapy protocol for most tumors delivers a total dose of 50–70 Gy in 2 Gy fractions on each weekday, with no treatment given on weekends. To reduce toxicity and increase efficiency, alternative treatments have been considered, including a hyperfractionated protocol with 1 Gy per fraction twice a day; an accelerated regimen of 1.2 Gy per fraction twice daily; and hypofractionation with 5 Gy twice-a-week fractions. Here, we develop a minimal mathematical model to study the effect of tumor heterogeneity and repair in tumors exposed to theses different radiation treatment schedules.

Several mathematical models have been developed to simulate the effects of radiotherapy. Most models utilize the so-called linear quadratic (LQ) model and its various extensions (Hall and Giaccia 2006). In the original LQ model, cell survival probability S after acute doses of radiation d can be estimated with
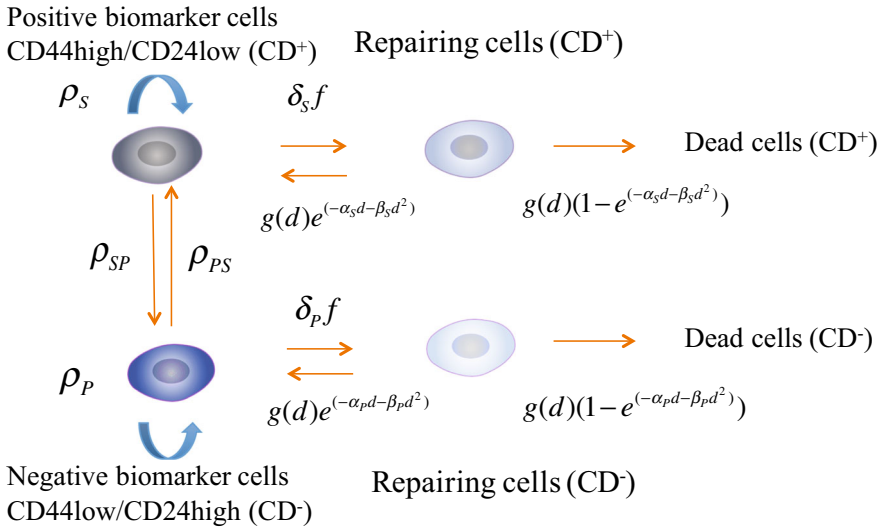
$$S(d) = \exp(-\alpha d - \beta d^2), \tag{1}$$

where α (Gy^{-1}) and β (Gy^{-2}) are tissue-specific radiosensitivity parameters that are usually derived from fitting the LQ model to clonogenic survival data (Hall and Giaccia 2006). More recently, mathematical frameworks have been combined with experimental data to investigate the different responses to clinically available radiation protocols (Dhawan et al. 2014; Dionysiou et al. 2004; Enderling et al. 2009; Stamatakos et al. 2014). Recently, Leder et al. (2014) proposed an optimized radiation dosing schedule for PDGF-driven glioblastoma. The model, however, is dependent on a large number of parameters and, with limited biological data, some parameters are far from biological realism. In particular, tissue-specific radiosenstivity parameters α and β are derived such that the derived ratio of $\alpha/\beta = 865, 789$ Gy is five orders of magnitude larger than frequently derived $\alpha/\beta = 3 - 10$ Gy (Leder et al. 2014). Nevertheless, the model-predicted optimal dose fractionation showed prolonged survival in subsequent mouse experiments, emphasizing that the currently applied standard-of-care radiation fractionation may not yield optimal outcomes. Mathematical models may help decipher the complex biology underlying cancer cell response to irradiation, with the ultimate aim to improve clinical application of radiotherapy.

Herein we propose a simple mathematical model of breast cancer cell dynamics under fractionated radiation exposure. The model includes phenotypic cell heterogeneity and plasticity, as well as radiation-induced cell cycle arrest, which may play a pivotal role in analyzing radiation protocols with multiple doses per day. The effect of different model parameters and repair mechanisms on heterogeneity are studied for different clinically feasible radiotherapy treatments.

2 Method

We developed a two-compartment mathematical model to analyze the effect of radiation therapy on the two phenotypically distinct subpopulations of radioresistant and radiosensitive cancer cells. In breast cancer, these populations have been identified by, respectively, CD44highCD24low (CD^{+}; biomarker positive) and CD44lowCD24high (CD^{-}; biomarker negative), which are also markers of cancer stemness (Al-Hajj et al. 2003; Fillmore and Kuperwasser 2008). Both subpopulations are capable of self-renewal, albeit with lower rates for biomarker negative CD^{-} cells that also feature higher death rates. We discuss the balance of self-renewal and cell death as the net population growth rate, which does not affect the behavior of the system. As a visualization of phenotypic plasticity, cells can switch from one phenotype to the other (Marjanovic et al. 2013). After exposure to radiation, cells in each compartment are forced into cell cycle arrest to attempt repair from radiation-induced DNA damage. Biomarker positive cells have been shown to have better repair mechanisms (Bao et al. 2006; Baumann et al. 2008) and, thus, a larger fraction of growth-arrested biomarker positive CD^{+} (calculated by the LQ model with phenotype-specific α_S and β_S parameters) returns into the viable population after successful repair. Figure 1 shows a schematic diagram of the proposed model, and model parameters are summarized in Table 1.

We denote by N_S, N_{RS}, N_P, and N_{RP} the population of resistant cells, resistant repairing cells, sensitive cells, and sensitive repairing cells, respectively. The model can be mathematically represented by the following system of equations

Positive biomarker cells
CD44high/CD24low (CD⁺)   Repairing cells (CD⁺)

ρ_S $\delta_S f$

Dead cells (CD⁺)

$g(d)e^{(-\alpha_S d - \beta_S d^2)}$ $g(d)(1 - e^{(-\alpha_S d - \beta_S d^2)})$

ρ_{SP} ρ_{PS}

$\delta_P f$

Dead cells (CD⁻)

ρ_P

$g(d)e^{(-\alpha_P d - \beta_P d^2)}$ $g(d)(1 - e^{(-\alpha_P d - \beta_P d^2)})$

Negative biomarker cells   Repairing cells (CD⁻)
CD44low/CD24high (CD⁻)

Fig. 1 (Color figure online) Schematic diagram of the model

Table 1 Description of the model parameters

Parameters	Description
ρ_S	Net proliferation rate of CD^+ cells
ρ_{SP}	Rate of switching of CD^+ cells to CD^- cells
ρ_P	Net proliferation rate of CD^- cells
ρ_{PS}	Rate of switching of CD^- cells to CD^+ cells
$\delta_S f$	Rate at which CD^+ cells go for repair
$\delta_P f$	Rate at which CD^- cells go for repair
$g(d)(1 - e^{(-\alpha_S d - \beta_S d^2)})$	Rate at which CD^+ cells that are in repair die
$g(d)(1 - e^{(-\alpha_P d - \beta_P d^2)})$	Rate at which CD^- cells that are in repair die
$g(d)e^{(-\alpha_S d - \beta_S d^2)}$	Rate at which CD^+ cells that are in repair become active again
$g(d)e^{(-\alpha_P d - \beta_P d^2)}$	Rate at which CD^- cells that are in repair become active again

$$
\begin{aligned}
\frac{dN_S}{dt} &= \rho_S N_S + \rho_{PS} N_P + g(d)e^{(-\alpha_S d - \beta_S d^2)} N_{RS} - \rho_{SP} N_S - \delta_S f N_S, \\
\frac{dN_{RS}}{dt} &= \delta_S f N_S - g(d) N_{RS}, \\
\frac{dN_P}{dt} &= \rho_P N_P + \rho_{SP} N_S + g(d)e^{(-\alpha_P d - \beta_P d^2)} N_{RP} - \rho_{PS} N_P - \delta_P f N_P, \\
\frac{dN_{RP}}{dt} &= \delta_P f N_P - g(d) N_{RP}.
\end{aligned}
\tag{2}
$$

Table 2 Fractionated irradition effect on CSC population and mammosphere formation capacity (Lagadec et al. 2010)

$CD24^{low/-}/CD44^{high}$		
Dose	% of CSCs	Sphere forming capacity
2	6.54 ($\pm$1.95)	13.49 ($\pm$ 1.32)
2–2	8.04 ($\pm$ 1.47)	10.76 ($\pm$ 0.96)
2–2–2–2	8.56 ($\pm$ 1.21)	11.85 ($\pm$ 1.81)
Overall average	7.71	12.03

Cells acquire on average one DNA double strand break after exposure to 1 Gy of radiation. Therefore, we assume that each cell will enter cell cycle arrest and attempt repair after each radiation fraction, but no new damage arises in the interval between radiation treatments. Hence, $f = 1$ at discrete times when radiation is given, and $f = 0$ otherwise. Dependent on radiosensitivity parameters α_i and β_i with $i \in \{S, P\}$, cells will either die due to radiation-induced DNA damage with probability $1 - S_i(d)$ or return to the viable non-repairing population S or P with probability $S_i(d)$ at dose-dependent rate $g(d)$. We assume the function $g(d)$ to be of the order of inverse square of the dose (Lagadec et al. 2010; Sarcar et al. 2011), such that cells irradiated with a dose of 1 Gy spend on average 1 h attempting repair, and 4 h after exposure to 2 Gy.

2.1 Parameter estimation

Stochastic and deterministic simulations have been compared to two sets of experimental data to derive suitable values for model parameters. The experimental study on breast cancer initiating cells (i.e., CSCs) and mammosphere formation assay (MFA) data calibrates the fraction of biomarker positive CSCs (Lagadec et al. 2010). In this study, the breast cancer cell line is irradiated with a single dose or daily doses of 2 Gy. After 48 hours, single cells are seeded to form spheres for 20 days. The fraction of CSCs and mammosphere formation capacity are reported in Table 2 (Lagadec et al. 2010).

As the MFA experiment was initiated from a single cell (Lagadec et al. 2010), stochastic effects are important. We apply the Gillespie algorithm to compare model sphere forming capacity predictions with the experimental data in Table 2. Since running the Gillespie algorithm is computationally expensive, it is only used to fit the parameters of the model when $\delta_s = \delta_p = g = 0$. We vary model parameters without repair to obtain the best fit to the experimental data. At the same time, we use the deterministic Eq. 2 to compare the theoretical results of average CSC fraction to experimental data. The estimated model parameters are summarized in Table 3, alongside the fraction of CSCs and sphere forming capacity using those values, which show good agreement with the experimental results in Table 2. Of note is that the reported parameter value combinations are not unique and, thus, we will perform a sensitivity analysis to investigate the impact of each parameter on model outcome.

Table 3 Estimated model parameters when $\delta_S = \delta_P = g = 0$

Parameters	ρ_S	ρ_{SP}	ρ_P	ρ_{PS}	% of CSCs	Sphere forming capacity
Values	0.2	0.7	0.1	0.05	7.6	12.7

The values of fraction of CSCs and sphere forming capacity that are evaluated based on the estimated parameters values are also reported. The unit of all parameters is $1/day$
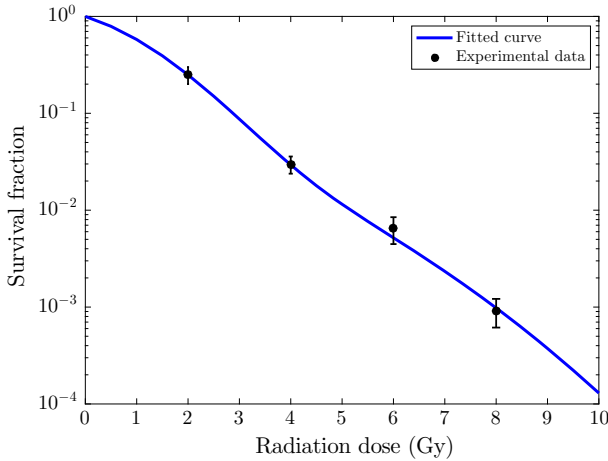
Fig. 2 (Color figure online) Fitting the modified linear quadratic model to the experimental data of (Phillips et al. 2006). The black points are the extracted experimental data. The solid curve is the model result using the estimated radiosensitivity parameters $\alpha_S = 0.14$ Gy^{-1}, $\beta_S = 0.048$ Gy^{-2}, $\alpha_P = 0.41$ Gy^{-1} and $\beta_P = 0.17$ Gy^{-2}

Herein, resistant and sensitive tumor cells are considered to have different radiosensitivities. Thus, the total population of cells at time t is given by $N(t) = N_S(t) + N_P(t)$ (hereafter, $N_S \equiv N_S + N_{RS}$ and $N_P \equiv N_P + N_{RP}$ unless stated otherwise); the population of cells after exposure to treatment for the period of time τ can be calculated as

$$\frac{N(t+\tau)}{N(t)} = \frac{N_S(t)}{N(t)} e^{(-\alpha_S d - \beta_S d^2)} + \frac{N_P(t)}{N(t)} e^{(-\alpha_P d - \beta_P d^2)}. \tag{3}$$

Assuming that the fraction of CSCs is at its steady-state value before the radiation, and using the experimental data of (Lagadec et al. 2010), we set $\frac{N_S(t)}{N(t)} = 0.076$ (and $\frac{N_P(t)}{N(t)} = 0.924$). Then, the modified linear quadratic model (Eq. 3) is used to fit model results to the experimental data of (Phillips et al. 2006), which yields $\alpha_S = 0.14$ Gy^{-1}, $\beta_S = 0.048$ Gy^{-2} (α_S/β_S=2.9 Gy), $\alpha_P = 0.41$ Gy^{-1} and $\beta_P = 0.17$ Gy^{-2} (α_S/β_S=2.4 Gy) (Fig. 2). Since at each radiation fraction the majority of damaged cells undergo repair mechanisms, we assume that 90% of cells will be arrested (Withers 1992). However, sensitivity analysis shows that reducing this fraction as low as to 40% does not qualitatively change the results (see Figure S1 and Figure S2 in supplementary materials). The list of all model parameters and their estimated values are reported in Table 4.

Table 4 Model parameter values

Parameters	Value (unit)	Reference
ρ_S	0.2 (day^{-1})	Using experimental data (Lagadec et al. 2010)
ρ_{SP}	0.7 (day^{-1})	Using experimental data (Lagadec et al. 2010)
ρ_P	0.1 (day^{-1})	Using experimental data (Lagadec et al. 2010)
ρ_{PS}	0.05 (day^{-1})	Using experimental data (Lagadec et al. 2010)
$\delta_S = \delta_P$	310 (day^{-1})	Assuming 90% of cancer cells undergo repair
α_S	0.14 (Gy^{-1})	Using experimental data (Phillips et al. 2006)
α_P	0.41 (Gy^{-1})	Using experimental data(Phillips et al. 2006)
β_S	0.048 (Gy^{-2})	Using experimental data (Phillips et al. 2006)
β_P	0.17 (Gy^{-2})	Using experimental data (Phillips et al. 2006)
f	1 or 0	1: radiation, 0: no radiation

3 Results

We consider different clinical radiotherapy treatment protocols for one week including standard of care (SoC; daily doses of 2 Gy), hyperfractionated (HR; two daily doses of 1 Gy), accelerated hyperfractionation (AC; two daily doses of 1.2 Gy), and hypofractionated (HO; twice-a-week doses of 5 Gy). Additionally, we simulate the recently suggested optimal protocol for PDGF-driven glioblastoma by Leder (Leder et al. 2014) (Optimum-1, OP; see Table 5). All protocols deliver a total dose of $D = 10$ Gy per week, except accelerated hyperfractionated with a total dose of $D = 12$ Gy. However, the accelerated hyperfractionated protocol has the same biologically effective dose (BED) as SoC (see Table 6). BED is used to describe the biological effect of dose fractionation and is defined as

$$\text{BED} = \frac{-\ln(SF(d))}{\alpha} = D\left(1 + \frac{d}{\alpha/\beta}\right), \tag{4}$$

where $SF(d)$ is the LQ model derived single dose d-dependent survival fraction with radiobiological parameters α and β (compare Eq. 1). Due to the linear quadratic relationship of dose and survival, total dose can be increased when smaller doses are given in each fraction (Fowler 1989). The model introduced in Sect. 2 considered two subgroups of cancer cells (resistant cells and sensitive cells) with different radiosensitivities. Thus, following the survival fraction of cancer cells in Eq. 3, the BED is given by

$$\text{BED} = \frac{-\ln(mSF_S + (1-m)SF_P)}{m\alpha_S + (1-m)\alpha_P}, \tag{5}$$

where SF_S and SF_P are survival fractions for resistant cells and sensitive cells, respectively. The constant m represents the proportion of resistant cells in the tumor prior to irradiation. Table 6 shows the BED for the standard of care (SoC), hyperfrac-

Table 5 Radiotherapy schedules for one week of treatment. Different colors are used for corresponding colors in the figures

Schedule	Day 1	Day 2	Day 3	Day 4	Day 5
Standard of care (SoC)	2	2	2	2	2
Hyperfractionated (HR)	2×1	2×1	2×1	2×1	2×1
Optimum-1 (OP)	3×1	1	2×1	1	3×1
Hypofractionated (HO)	5	–	–	–	5
Accelerated hyperfractionated (AC)	2×1.2	2×1.2	2×1.2	2×1.2	2×1.2

Table 6 Biological effective dose for hyperfraction, standard of care, and accelerated hyperfractionated protocols

| BED	Schedules		
	HR ($d = 1, n = 10$)	SoC ($d = 2, n = 5$)	AC ($d = 1.2\, n = 10$)
BED_S ($m = 1$)	13.5	17.1	17.1
BED_P ($m = 0$)	14.1	18.3	17.9
BED_{SP} ($m = 0.076$)	11.1	12.7	12.7

tionated (HR), and accelerated hyperfractionated (AC) protocols with different initial fractions of resistant cells: tumors containing only resistant cells ($m = 1$), tumors containing only sensitive cells ($m = 0$), and heterogeneous tumors with a small sub-population of resistant cells ($m = 0.076$) as estimated. The BED is almost identical for standard-of-care and accelerated hyperfractionation, but significantly smaller for hyperfractionation.

Figure 3 shows the number of cancer cells $N_S + N_P$ and fraction of resistant cells $N_S/(N_S + N_P)$ for all considered radiation schedules (compare Table 5). Simulations show that protocols with larger number of fractions leads to more cell kill, with accelerated hyperfractionation yielding the smallest number of cells after one week of therapy. However, the fraction of stem cells is largest compared to the other radiotherapy protocols. Hypofractionation with smallest overall cell kill leads also to least competitive release of the most resistant stem cell subpopulation (Enderling et al. 2009).

For the chosen parameter combinations (Table 4), accelerated hyperfractionation and SoC schedules yield the lowest number of cancer cells after one week of treatment (Fig. 3). Sensitivity analysis showed that the results are robust to changes in the parameter values (Table 7), with the exception that decreasing α_P and β_P by 50% produces hypofractionated and accelerated hyperfractionated as best protocols (Fig. 4).

Heretofore we assumed that 90% of cells undergo arrest to attempt repair, and the parameter values for δ_S and δ_P were chosen large enough to satisfy this assumption. However, decreasing the values for these parameters so that less than 40% of cells attempt repair suggests accelerated hyperfractionated as the best schedule (see Figure
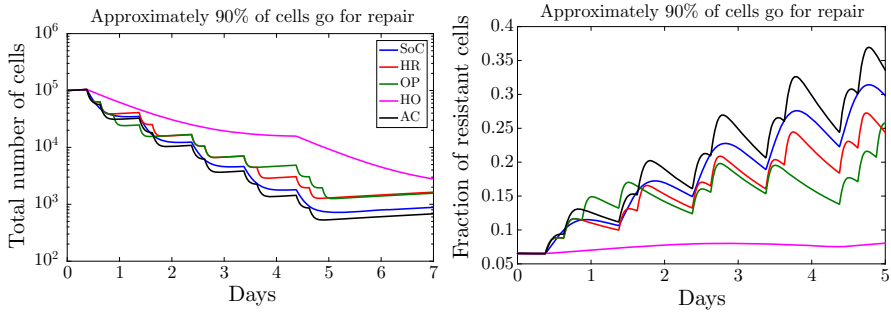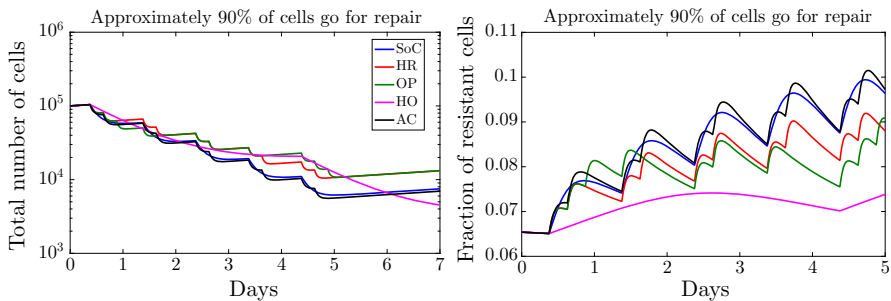
Fig. 3 (Color figure online) Number of cancer cells $N_S + N_P$ and the fraction of resistant cells $N_S/(N_S + N_P)$ for radiotherapy protocols reported in Table 5

Table 7 Sensitivity analysis for different parameters of the model

Parameters	α_S, β_S	α_P, β_P	ρ_S	ρ_P	ρ_{PS}	ρ_{SP}	1st best	2st best
Default	0.14, 0.05	0.41, 0.17	0.2	0.1	0.044	0.73	AC	SoC
α_S, β_S (+50%)	0.21, 0.07	0.41, 0.17	0.2	0.1	0.044	0.73	AC	SoC
α_S, β_S (−50%)	0.07, 0.04	0.41, 0.17	0.2	0.1	0.044	0.73	AC	SoC
α_P, β_P (+50%)	0.14, 0.05	0.61, 0.25	0.2	0.1	0.044	0.73	AC	SoC
α_P, β_P (−50%)	0.14, 0.05	0.21, 0.08	0.2	0.1	0.044	0.73	HO	AC
ρ_S (+50%)	0.14, 0.05	0.41, 0.17	0.3	0.1	0.044	0.73	AC	SoC
ρ_S (−50%)	0.14, 0.05	0.41, 0.17	0.1	0.1	0.044	0.73	AC	SoC
ρ_P (+50%)	0.14, 0.05	0.41, 0.17	0.2	0.15	0.044	0.73	AC	SoC
ρ_P (−50%)	0.14, 0.05	0.41, 0.17	0.2	0.05	0.044	0.73	AC	SoC
ρ_{PS} (+50%)	0.14, 0.05	0.41, 0.17	0.2	0.1	0.066	0.73	AC	SoC
ρ_{PS} (−50%)	0.14, 0.05	0.41, 0.17	0.2	0.1	0.022	0.73	AC	SoC
ρ_{SP} (+50%)	0.14, 0.05	0.41, 0.17	0.2	0.1	0.044	1.09	AC	SoC
ρ_{SP} (−50%)	0.14, 0.05	0.41, 0.17	0.2	0.1	0.044	0.36	AC	SoC

Fig. 4 (Color figure online) Number of cancer cells $N_S + N_P$ and the fraction of resistant cells $N_S/(N_S + N_P)$ when α_P and β_P are changed to $\alpha_P - 0.5\alpha_P$ and $\beta_P - 0.5\beta_P$ for radiotherapy protocols reported in Table 7

S1 and Figure S2 in supplementary materials). Furthermore, the model considers that cells leave arrest with rate $g(d)$, which is assumed to be on the order of $1/\text{dose}^2$. If $g(d)$ was proportional to $1/\text{dose}$ the number of cancer cells at the end of the course of radiation therapy decreases significantly; however, the accelerated hyperfractionated schedule remains the best treatment protocol followed by SoC. Moreover, if $g(d) = 1$, the order of the best treatment regimens remains (see Figures S3, S4, and S5 in supplementary materials).

4 Conclusion

In this paper, a two-compartment mathematical model has been developed to assess the effect of tumor heterogeneity and radiotherapy fractionation on treatment response. Model simulations suggest that radiotherapy can alter tumor heterogeneity and elevates the fraction of resistant cells. Future studies may further increase biological complexity by considering increased self-renewal of the resistant population in response to radiation (Gao et al. 2013). If the total radiation dose is insufficient to eradicate the tumor, enrichment in cancer stem cells may lead to tumor relapse and recurrence. Therefore, if total tumor control cannot be achieved optimal therapies should balance decreases in tumor burden and prevention of outgrowth of the most resistant subpopulation. Interestingly, none of our simulations suggested standard-of-care fractionation as the best therapeutic approach, further emphasizing the need to prospectively evaluate alternative fractionation protocols in the clinic. Furthermore, our model calibrated for breast cancer was unable to confirm the optimum treatment schedule for PDGF-driven glioblastoma (as in Leder et al. 2014). This suggests that treatment optimization may be highly tumor biology, mathematical model, and model parameter dependent, and utmost importance must be paid to identifying underlying biological mechanisms. Hence, a general optimal radiation schedule as suggested in (Conforti et al. 2008; Leder et al. 2014; Wein et al. 2000) may not be feasible and designing an efficient protocol may be required for each type of cancer, and even each individual patient.

At the moment, the study is hypothesis generating, and we sincerely hope that the presented results are exciting and encouraging for experimentalists and clinicians to test the presented model predictions.

References

Al-Hajj Muhammad, Wicha Max S, Benito-Hernandez Adalberto, Morrison Sean J, Clarke Michael F (2003) Prospective identification of tumorigenic breast cancer cells. Proc Nat Acad Sci 100(7):983–3988

Bao Shideng, Qiulian Wu, McLendon Roger E, Hao Yueling, Shi Qing, Hjelmeland Anita B, Dewhirst Mark W, Bigner Darell D, Rich Jeremy N (2006) Glioma stem cells promote radioresistance by preferential activation of the DNA damage response. Nature 444:756–760

Baumann Michael, Krause Mechthild, Hill Richard (2008) Exploring the role of cancer stem cells in radioresistance. Nat Rev Cancer 8:545–554

Conforti Domenico, Guerriero Francesca, Guido Rosita (2008) Optimization models for radiotherapy patient scheduling. 4OR 6:263–278

Dhawan Andrew, Kohandel Mohammad, Hill Richard, Sivaloganathan Sivabal (2014) Tumour control probability in cancer stem cells hypothesis. PLoS ONE 9:e96093

Dionysiou Dimitra D, Stamatakos Georgios S, Uzunoglu Nikolaos K, Nikita Konstantina S, Marioli Antigoni (2004) A four-dimensional simulation model of tumour response to radiotherapy in vivo: parametric validation considering radiosensitivity, genetic profile and fractionation. J Theor Biol 230:1–20

Enderling Heiko, Park Derek, Hlatky Lynn, Hahnfeldt Philip (2009) The importance of spatial distribution of stemness and proliferation state in determining tumor radioresponse. Math Model Nat Phenom 4:117–133

Enderling Heiko, Anderson Alexander RA, Chaplain Mark AJ, Beheshti Afshin, Hlatky Lynn, Hahnfeldt Philip (2009) Paradoxical dependencies of tumor dormancy and progression on basic cell kinetics. Cancer Res 69(22):8814–8821

Fillmore Christine M, Kuperwasser Charlotte (2008) Human breast cancer cell lines contain stem-like cells that self-renew, give rise to phenotypically diverse progeny and survive chemotherapy. Breast Cancer Res 10(2):1

Fowler John F (1989) The linear-quadratic formula and progress in fractionated radiotherapy. Br Jo Radiol 62:679–694

Gao Xuefeng, McDonald John T, Hlatky Lynn, Enderling Heiko (2013) Acute and fractionated irradiation differentially modulate glioma stem cell division kinetics. Cancer Res 73(5):1481–1490

Gupta Piyush B, Fillmore Christine M, Jiang Guozhi, Shapira Sagi D, Tao Kai, Kuperwasser Charlotte, Lander Eric S (2011) Stochastic state transitions give rise to phenotypic equilibrium in populations of cancer cells. Cell 146:633–644

Hall Eric J, Giaccia Amato J (2006) Radiobiology for the radiologist. Lippincott Williams and Wilkins, Philadelphia

Haviland Joanne S, Owen J Roger, Dewar John A, Agrawal Rajiv K, Barrett Jane, Barrett-Lee Peter J, Dobbs H Jane et al (2013) The UK Standardisation of Breast Radiotherapy (START) trials of radiotherapy hypofractionation for treatment of early breast cancer: 10-year follow-up results of two randomised controlled trials. Lancet Oncol 14:1086–1094

Lagadec Chann, Vlashi Erina, Della Donna Lorenza, Meng YongHong, Dekmezian Carmen, Kim Kwanghee, Pajonk Frank (2010) Survival and self-renewing capacity of breast cancer initiating cells during fractionated radiation treatment. Breast Cancer Res 12:R13

Leder Kevin, Pitter Ken, LaPlant Quincey, Hambardzumyan Dolores, Ross Brian D, Chan Timothy A, Holland Eric C, Michor Franziska (2014) Mathematical modeling of PDGF-driven glioblastoma reveals optimized radiation dosing. Cell 156:603–616

Mathews Lesley A, Cabarcas Stephanie M, Hurt Elaine M (2013) DNA repair of cancer stem cells. Springer, Berlin

Marjanovic Nemanja D, Weinberg Robert A, Chaffer Christine L (2013) Cell plasticity and heterogeneity in cancer. Clin Chem 59:168–179

Phillips Tiffany M, McBride William H, Pajonk Frank (2006) The response of CD24-/low/CD44+ breast cancer initiating cells to radiation. J Natl Cancer Inst 98:1777–1785

Reya Tannishtha, Morrison Sean J, Clarke Michael F, Weissman Irving L (2001) Stem cells, cancer, and cancer stem cells. Nature 414:105–111

Sarcar Bhaswati et al (2011) Targeting radiation-induced G2 checkpoint activation with the Wee-1 inhibitor MK-1775 in glioblastoma cell lines. Mol Cancer Ther 10:2405–2414

Stamatakos GS, Antipas VP, Uzunoglu NK, Dale RG (2014) A four-dimensional computer simulation model of the in vivo response to radiotherapy of glioblastoma multiforme: studies on the effect of clonogenic cell density. Br J Radiol 79:389

Shackleton Mark, Quintana Elsa, Fearon Eric R, Morrison Sean J (2009) Heterogeneity in cancer: cancer stem cells versus clonal evolution. Cell 138:822–829

Trialists' Group (2008) The START, The UK Standardisation of Breast Radiotherapy (START) Trial B of radiotherapy hypofractionation for treatment of early breast cancer: a randomised trial. Lancet 371:1098–1107

Wein Lawrence M, Cohen Jonathan E, Wu Joseph T (2000) Dynamic optimization of a linear-quadratic model with incomplete repair and volume-dependent sensitivity and repopulation. Int J Radiat Oncol Biol Phys 47:1073–1083

Withers HR (1992) Biological basis of radiation therapy for cancer. Lancet 339(8786):156–9